

Estimating the Contribution of Woodsmoke to Winter-time PM_{2.5} Levels Along the Wasatch Front

Jesse Glisson¹, Nancy Daher², Adrian Wride¹, Alex Robinson¹, Kerry Kelly¹

¹Department of Chemical Engineering, University of Utah, Salt Lake City, Utah, USA

²Division of Air Quality, Utah Department of Environmental Quality, Salt Lake City, Utah, USA

December 31, 2019

Several counties along Utah's Wasatch Front are designated as EPA nonattainment areas for particulate smaller than 2.5 microns (PM_{2.5}) due to elevated PM_{2.5} levels associated with winter-time persistent cold air pools (PCAPs). To reduce particulate emissions during PCAPs, the Utah Division of Air Quality (DAQ) issues mandatory and voluntary no-burn days, during which residential solid-fuel burning is restricted. This study combined stationary and mobile monitoring strategies to estimate the contribution of commercial and residential wood-burning to local PM_{2.5} concentrations and to assess compliance with wood-burning restrictions. It employed a seven-wavelength optical absorption aethalometer to qualitatively measure the presence of wood smoke particulate material (WS PM) using Delta-C, which is the difference between light attenuation at 370 nm relative to 880 nm. The resulting Delta-C values are being compared to regulatory PM_{2.5} measurements, heat deficit, and whether burn restrictions were issued. Mobile monitoring was performed by driving a predetermined route during both burn and no-burn days in January and February 2018. This was performed using a real-time aerosol monitor (DustTrak II 8350), an aethalometer (Magee Scientific AE33), and a handheld GPS unit (Garmin eTrex-20X). The mobile monitoring route included areas of known residential and commercial wood-burning and resulted in maps that provide a strong indication of the effect of local wood-burning sources on PM_{2.5} levels. The results indicate several commercial and residential locations consistently burn wood regardless of DAQ restrictions.

Contents

Abstract	1
Background and Significance	4
Purpose	4
Stationary Monitoring	5
Mobile Monitoring	5
Methods and Materials	5
Aethalometer (Magee Scientific Aethalometer Model AE33)	5
PM _{2.5} Aerosol Monitor (DustTrak II 8350)	7
Stationary Monitoring	8
Mobile Monitoring	10
Deviations	18
Results	19
Stationary Monitoring	19
Mobile Monitoring	23
Conclusions	26
Data Archive	27
Online Delta Carbon Tool	27
Future Direction	27
Data Management	28
References	29
Appendices	
Appendix A: Aethalometer Parameters for Delta-C Calculation	
Appendix B: Mobile Monitoring	
Appendix B.1: Mobile Monitoring Dates	
Appendix B.2: PM _{2.5} and Delta-C Mobile Monitoring Plots	
Appendix C: Stationary Monitoring	
Appendix C.1: Delta-C and Heat Deficit	
Appendix C.2: Delta-C and PM _{2.5}	

Appendix C.3: Delta-C and Temperature

Background and Significance

The valleys along Utah's Wasatch Front experience periods of elevated PM_{2.5} levels during winter-time PCAPs caused by topographical features, weather patterns, primary aerosol emissions, and secondary aerosol formation. The strength of PCAPs can be measured using heat deficit, which can also serve as an indication of whether a PCAP is building, being maintained, or being destroyed.¹ PM_{2.5} concentrations have been observed to increase with both the intensity and duration of PCAPs in the Salt Lake Valley.² As a result, the Environmental Protection Agency (EPA) has designated six counties in Utah (Box Elder, Davis, Salt Lake, Tooele, Utah, and Weber Counties) as "serious non-attainment areas" for PM_{2.5}, and Cache County as a "moderate non-attainment area" for PM_{2.5} for failure to achieve the 2006 federal 24-hour National Ambient Air Quality Standards (NAAQS) of 35 $\mu\text{g}/\text{m}^3$. Elevated levels of PM_{2.5} contribute to numerous respiratory health problems and adverse health effects.³ Elevated levels of PM_{2.5} pose a greater risk than larger particulate matter because it can penetrate deeply into the lungs causing inflammation and damage to lung tissue.⁴ A study in Vancouver concluded that woodsmoke particles are 7 times more likely to enter a person's lungs than the average PM_{2.5} particle in Vancouver's air.⁵ The increased likelihood of inhalation can be attributed to wood-burning particles being significantly smaller than 2.5 microns, averaging only 38 nm.⁶ For this same reason, wood smoke particulate is also more likely to seep into surrounding homes, with indoor black carbon (BC) levels averaging 78% of outdoor levels.⁷

Wood-burning is a significant contributor to PM_{2.5} levels along the Wasatch Front during wintertime PCAPs. A four-year study conducted in three Utah cities: Bountiful, Salt Lake City, and Lindon from 2007 to 2011 determined that 5-10% of the total PM_{2.5} contribution resulted from wood smoke during days when PM_{2.5} mass exceeded 30 $\mu\text{g}/\text{m}^3$.⁸ Similarly, wood smoke and cooking were shown to contribute 20-70% of primary PM_{2.5} emissions in Bountiful, Utah when PM_{2.5} levels exceeded 20 $\mu\text{g}/\text{m}^3$.⁹ In attempt to mitigate particulate emissions during periods of reduced air quality, the Utah Division of Air Quality (DAQ) implements varying wood-burning restrictions; however, compliance with these restrictions is uncertain. Restaurants and institutional food preparation facilities are currently exempt from these no-burn restrictions under Utah Administrative Rule R307-302-2. The EPA and the California Air Resources Board report that the inhalable particulate pollution from a single wood stove is equivalent to roughly 3,000 times the particulate pollution from a gas furnace that produces the same amount of heat per unit. In 2017, Gov. Gary Herbert announced plans to reduce Utah's emissions by 25% by 2026. Consequently, implementing more effective wood-burning restrictions could help meet goals for reducing ambient PM_{2.5} levels.

Purpose

Stationary Monitoring

Stationary monitoring was performed in an effort to understand the contribution of wood-burning to PM_{2.5} levels at key monitoring stations along the Wasatch Front, and to assess how this contribution is affected by temperature, heat deficit, and residential wood-burning restrictions. This study aimed to understand levels of compliance with wood-burning restrictions by examining the correlation between these restrictions and PM_{2.5} emissions from wood-burning sources.

Mobile Monitoring

Mobile monitoring strategies were employed in attempt to understand the contribution of commercial and residential wood-burning sources to PM_{2.5} levels in Salt Lake City, and to assess compliance with residential wood-burning restrictions.

Methods and Materials

Aethalometer (Magee Scientific Aethalometer Model AE33)

The incomplete combustion of carbonaceous fuels produces soot particles with strong optical absorption properties commonly referred to as black carbon (BC).¹⁰ The particle size and optical absorption properties of BC vary depending on a number of conditions including particle size, combustion fuel type, combustion conditions, and particle age. During a severe winter pollution event in Xi'an, China, BC particle sizes varied from 18.5 to 532.5 nm,¹¹ while other studies have found particle sizes above 660 nm.¹² A similar study in Beijing showed the highest occurrence of particle diameter to be 199 nm on clean days, and 221 nm on polluted days.¹³ This is consistent with the expectation that new BC particles are relatively small and grow under stable atmospheric conditions as they age.¹⁴

This study employed a Magee Scientific Model AE33 aethalometer for stationary and mobile monitoring. The seven-wavelength aethalometer operates by pulling an air stream through a filter tape, and as BC particles accumulate on the filter tape, the optical transmission through the filter is reduced. From the rate of decrease in optical transmission, the rate of increase in optical attenuation (ATN) can be calculated, which is proportional to the rate of BC loading. The AE33 incorporates a DualSpot™ measurement method, which measures the optical transmission through both a clean section of filter using a reference sensor, and through the section of

filter affected by aerosol loading. Optical attenuation at each wavelength (λ , nm) is defined as:

$$ATN(\lambda) = 100 * \ln \left(\frac{I_0(\lambda)}{I(\lambda)} \right) \quad (1)$$

where $I_0(\lambda)$ is the light intensity transmitted through the reference spot, and $I(\lambda)$ is the transmitted intensity through the section of filter affected by aerosol loading. The flow rate (Q , L min⁻¹) is measured within the instrument, and was verified by using a Gilibrator. From the flow rate and optical attenuation, the wavelength-dependent attenuation coefficient ($b_{atn}(\lambda)$) is calculated by:

$$b_{atn}(\lambda) = \frac{A * (\Delta ATN(\lambda))}{100 * Q \Delta t} \quad (2)$$

where A (cm²) is the spot area through which the optical attenuation is being measured, $\Delta ATN(\lambda)$ is the change in attenuation at a given wavelength during time period Δt .¹⁰ From the optical attenuation coefficient, the optical absorption coefficient ($b_{abs}(\lambda)$) is calculated by:

$$b_{abs}(\lambda) = \frac{b_{atn}(\lambda)}{C} \quad (3)$$

where $b_{atn}(\lambda)$ is the wavelength-specific attenuation coefficient.¹⁵ The wavelength scattering parameter ($C = 1.57$) was established based on the use of a TFE-coated glass fiber filter.¹⁶ The measured black carbon concentration ($BC_0(\lambda)$) is defined as:

$$BC_0(\lambda) = \frac{b_{abs}(\lambda)}{\sigma_{air}(\lambda)} \quad (4)$$

where $\sigma_{air}(\lambda)$ is the mass absorption cross-section (m² g⁻¹). The mass absorption cross-sections used for the $BC(\lambda)$ calculations at each corresponding wavelength can be found in Appendix A.¹⁷ The measured black carbon concentration must be corrected using the wavelength-specific loading compensation parameter $k(\lambda)$, which is calculated by the instrument for each filter spot and set to range from 0.015 to -0.005 as recommended by the manufacturer.^{17,18} This correction is performed to obtain the actual black carbon concentration ($BC(\lambda)$, ng m⁻³):

$$BC(\lambda) = \frac{BC_0(\lambda)}{(1 - k(\lambda)) * ATN(\lambda)} \quad (5)$$

Therefore, the concentration of black carbon is calculated by:

$$BC(\lambda) = \frac{A * \Delta ATN(\lambda)}{100 * Q * \sigma_{air}(\lambda) * C * (1 - k(\lambda)) * ATN(\lambda) * \Delta t} \quad (6)$$

which can be simplified to yield

$$BC(\lambda) = \left[\frac{A * \Delta ATN(\lambda)}{100 * \sigma_{air}(\lambda)} \right] * \left[\frac{1}{Q * \Delta T} \right] \quad (7)$$

It should be noted that The Magee Scientific AE33 measures the optical attenuation at seven wavelengths ranging from ultraviolet (370 nm) to infrared (950 nm), and simultaneously calculates a corresponding $BC(\lambda)$ value at each. The data obtained from channel 6 at 880 nm ($BC6$) is considered to be a defining standard for black carbon concentration:¹⁷

$$\text{Black carbon concentration: } BC = BC6 \quad (8)$$

The combustion of biomass such as wood-burning produces light absorbing organic particles referred to as brown carbon (BrC). While black carbon has been shown to absorb uniformly at all seven wavelengths, brown carbon exhibits increased attenuation at higher frequencies, specifically the 370 nm wavelength.¹⁹ Therefore, a parameter known as Delta-C (ng/m^3) can be used as an indicator of biomass combustion.^{20,21} Delta-C is defined as:

$$\text{Delta-C} = BC1 - BC6 \quad (9)$$

where $BC1$ and $BC6$ correspond to the data obtained from channel 1 (370 nm) and channel 6 (880 nm), respectively. It should be noted that although Delta-C is reported in units of ng/m^3 , an appropriate scaling factor must be applied to obtain a quantitative estimate of wood smoke $\text{PM}_{2.5}$ concentrations. The mass proportionality scaling factor varies significantly depending on combustion conditions, aerosol particulate age, and composition. One study determined a scaling factor of 15, while another study deduced a factor of 7.8.^{20,22} Due to this uncertainty, the Delta-C values in this study are reported for qualitative purposes rather than quantitative wood smoke $\text{PM}_{2.5}$ concentrations.

$\text{PM}_{2.5}$ Aerosol Monitor (DustTrak II 8350)

Mobile $\text{PM}_{2.5}$ measurements were obtained using a single-channel photometric DustTrak II 8350 Aerosol Monitor which measures real-time mass concentration of aerosols. This operates by passing a continuous aerosol stream through an impactor before entering a sensing chamber where it is illuminated by a sheet of laser light from a laser diode. To selectively sample only particulate less than 2.5 microns in diameter, the $\text{PM}_{2.5}$ impactor was used. The illuminated sheet of light then passes through a series of lenses before being focused onto a photo detector by a gold-coated spherical mirror. The voltage across the photo detector is proportional to the mass concentration of the aerosol. Prior to the study, the DustTrak was calibrated by the manufacturer (TSI, Inc.). Before deploying the instrument for mobile sample collection, the DustTrak was

co-located at a DAQ monitoring station from January 10 to January 15, 2019 to obtain a correction factor for local pollution conditions in the Salt Lake Valley. The linear regression used to obtain the correction factor is seen in Figure 1.

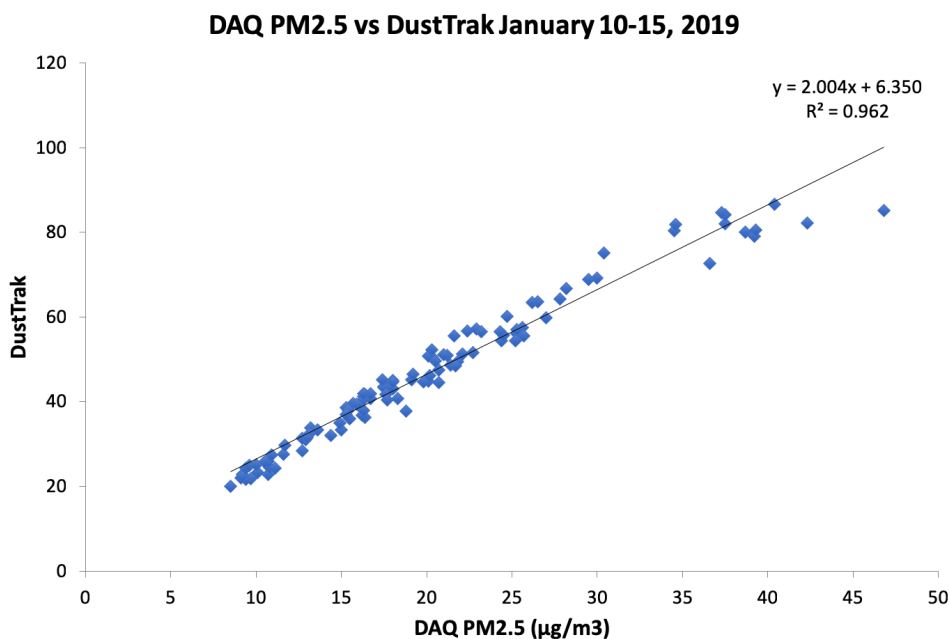


Figure 1: Linear regression of DAQ’s Thermo Scientific Model 5030i SHARP particulate monitor measurement of PM_{2.5} vs. the DustTrak measurement of PM_{2.5}. This regression provided the DustTrak’s correction factor.

Stationary Monitoring

Stationary monitoring occurred at four DAQ air monitoring stations along the Wasatch Front (Bountiful, Lindon, Rose Park, and Smithfield) from December 1, 2018 through February 28, 2019 (Figure 2). In addition to the standard instrumentation deployed at the DAQ monitoring stations, these four locations housed a Magee Scientific Aethalometer[®] Model AE33. The inlet to each aethalometer was connected to the glass air sampling manifold using antistatic tubing to prevent sample loss due to static effects. Each instrument sampled using a 60 second time base and 5 LPM flow rate, and was set to advance the filter tape once a maximum attenuation value of ‘24’ was reached. The glass air sampling manifold at Rose Park was damaged prior to the commencement of the stationary monitoring, which resulted in the sampling of a mixture of indoor and outdoor air. Because this mixture was not representative of outdoor ambient conditions, the data from the Rose Park station was not further analyzed.

To facilitate remote data collection, the DAQ hosts a publicly available data set of the hourly-averaged aethalometer data from each monitoring location. A python script was developed to automatically query this resource and regularly downloaded the data as the study progressed. Another python script was written to



Figure 2: Stationary monitoring locations

calculate and plot the Delta-C values for specified time periods. The Delta-C values were then compared to various data provided by the DAQ including temperature, $PM_{2.5}$ concentrations, and wood-burning restrictions. The Delta-C data was further analyzed and plotted alongside heat deficit values corresponding to the Salt Lake Valley. Heat deficit was calculated using data obtained from twice-daily rawinsonde launches near the Salt Lake City Airport. Heat deficit (H_h , $MJ m^{-2}$) is calculated as:²³

$$H_h = c_p \int_{1288m}^h \rho(z)[\theta_h - \theta(z)]dz \quad [J m^{-2}] \quad (10)$$

where c_p is the specific heat of air at constant temperature ($1005 J kg^{-1} K^{-1}$), θ_h is the potential temperature at height h (K), and $\rho(z)$ and $\theta(z)$ are the air density ($kg m^{-3}$) and potential temperature (K) from the rawinsonde sounding, and dz is the height interval between measurements of the rawinsonde soundings. The density (ρ) was not a measured parameter of the rawinsonde soundings and therefore was calculated using the Ideal Gas Law and the specific gas constant of dry air ($R_{air} = 287.06 J kg^{-1} K^{-1}$)

$$PV = mR_{air}T \quad (11)$$

where P is pressure (millibar), V is volume in m^3 , m is mass (kg), and T is temperature (K). The Ideal Gas

Law can be rearranged to solve for density by

$$\rho = \frac{m}{V} = \frac{P}{R_{air} * T} \quad (12)$$

The heat deficit was calculated from the Salt Lake Valley floor (1288 m) to $h = 2200$ m MSL as this is the approximate elevation of the Oquirrh Mountain ridgelines, which form the western boundary of the valley.²³ The potential temperature at height h ($\theta(h)$) is defined as the temperature a parcel of air would attain if it were adiabatically brought to a standard reference pressure (P_0) of 1000 millibars, and can be calculated by Poisson's Equation:

$$\theta(h) = T(h) \left(\frac{P_0}{P(h)} \right)^{R_{air}/c_p} \quad (13)$$

where $T(h)$ and $P(h)$ are the temperature (Kelvin) and pressure (millibar) at height h . In the event that the rawinsonde soundings did not have measurements at exactly 2200 m, the pressure and temperature values were calculated by linearly interpolating rawinsonde data to obtain approximate values.

Mobile Monitoring

A Magee Scientific Aethalometer Model AE33, DustTrak II 8350 Aerosol Monitor, and Garmin eTrex 20x handheld GPS were used simultaneously for mobile sampling. The DustTrak and AE33 were fastened to the floor immediately behind the driver seat in a van provided by the DAQ, positioned to minimize the necessary length of inlet tubing, and powered by a 12v DC to 120v AC inverter. Both the AE33 and DustTrak used 1/4" conductive copper tubing (to prevent static charge) connected to their inlets by a small section of antistatic tubing. The copper tubing for both instruments was routed out of the driver window with a gentle bend so that the sample inlets were pointed toward the rear of the vehicle, similar to a project performed by project completed by previous University of Utah chemical engineering students.²⁴ The tubing for both instruments terminated inside the narrow portion of a plastic funnel, with the larger funnel opening also pointed toward the rear of the vehicle. The funnel was implemented to reduce turbulent effects from causing particle dispersion or the disruption of continuous sampling. The Garmin GPS was placed on the vehicle dashboard to facilitate satellite communication. All three instruments sampled at 1-second intervals, were time-synced prior to each use, and the AE33 and DustTrak both used volumetric flow rates of 5 LPM. Once powered on, the AE33 took about 30 minutes to initialize and produce relatively stable readings, while the DustTrak and Garmin began collecting data almost immediately. Once the AE33 had stabilized, a match was lit near the inlet prior to driving to ensure that the DustTrak and AE33 data files aligned properly. This allowed for adjustments to subsequent data files to compensate for discrepancies between flow rates, tubing lengths, and measurement delays intrinsic to each instrument.

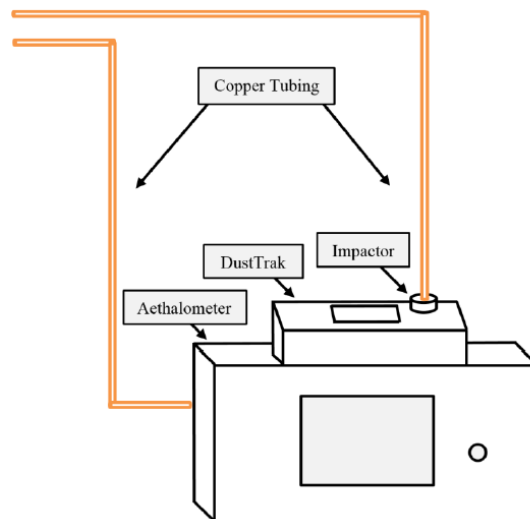


Figure 3: Mobile Monitoring System²⁴

Mobile sampling occurred on 12 evenings over a predetermined driving route that required roughly 3.5 hours to complete (January 16 to February 12, 2019). For continuity between sampling dates, driving generally occurred between 6 to 10 pm. The dates of monitoring were chosen in attempt to capture a distribution of various days of the week, air quality conditions, and residential wood-burning restrictions. A complete list of the mobile monitoring dates and corresponding day of the week, Salt Lake County wood-burning restrictions, and heat deficit can be found in Appendix B.1. The Salt Lake County Health Department provided a list of known commercial locations that use wood-burning for food preparation. This list was further refined to include locations that advertised wood-burning such as wood-fired pizza ovens. The mobile monitoring route was chosen to allow for sampling near the majority of the commercial wood-burning locations in Salt Lake County, while also sampling throughout some areas believed to contain frequent residential wood-burning. In the event that wood smoke was smelled or seen, the time and location was noted and minor route deviations ensued in attempt to locate the source. Whenever local traffic patterns allowed, the driving speed while sampling was kept below 20 MPH to reduce turbulent effects. The mobile monitoring route can be seen in Figure 4. The data was broken into different regions (denoted by colored blocks) for further analysis to determine trends between different areas in the Salt Lake County. These regions were largely defined using existing municipality boundaries.

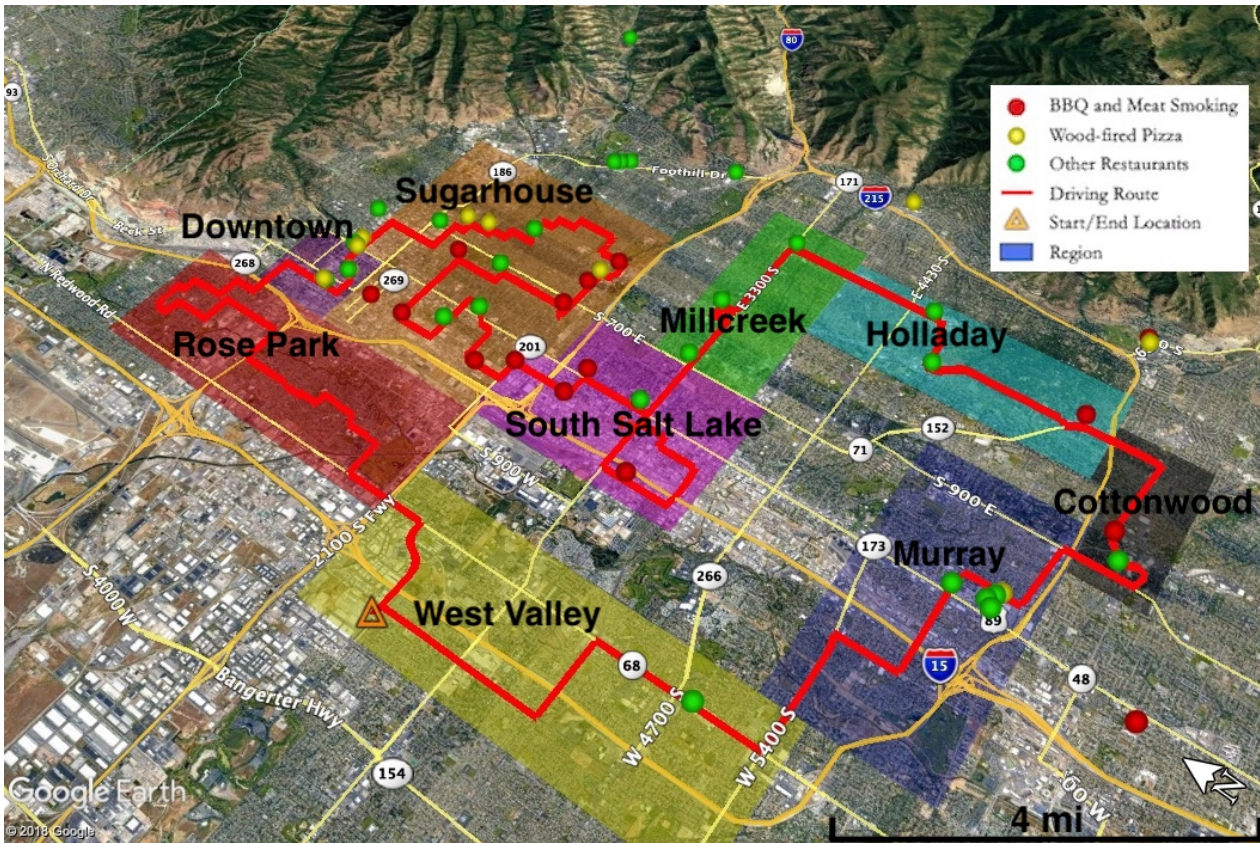


Figure 4: Mobile Monitoring Route

Before the data collected by mobile monitoring could be analyzed, several post-processing adjustments were necessary. Several of the mobile sampling periods had lower ambient $PM_{2.5}$ levels than encountered when the DustTrak was co-located at the DAQ monitoring station. Therefore, when the correction factor was applied to the DustTrak data, some of corrected values were negative and were subsequently set to zero. Because the aethalometer data is intrinsically noisy, a smoothing factor was applied. According to Tony Hansen at Magee Scientific, this smoothing factor is necessary when sampling at 1-second intervals to reduce noise and increase sensitivity. The manufacturer recommended to apply a fairly large smoothing factor such as 5-minute averaging, however, this would omit the desired spacial and temporal resolution. Therefore, a smoothing factor of '8' was applied throughout the aethalometer data set, as recommended by Tony Hansen. The smoothing factor corresponds to the size of the window with which a centered moving average was calculated on either side of a given value. For each driving date, both Delta-C and $PM_{2.5}$ data was then processed using a MATLAB script to produce .kmz files that could be viewed in Google Earth as geospatial plots to provide a visual representation of the mobile monitoring data. The $PM_{2.5}$ concentrations obtained from the January 16, 2019 mobile monitoring are shown in Figure 5.

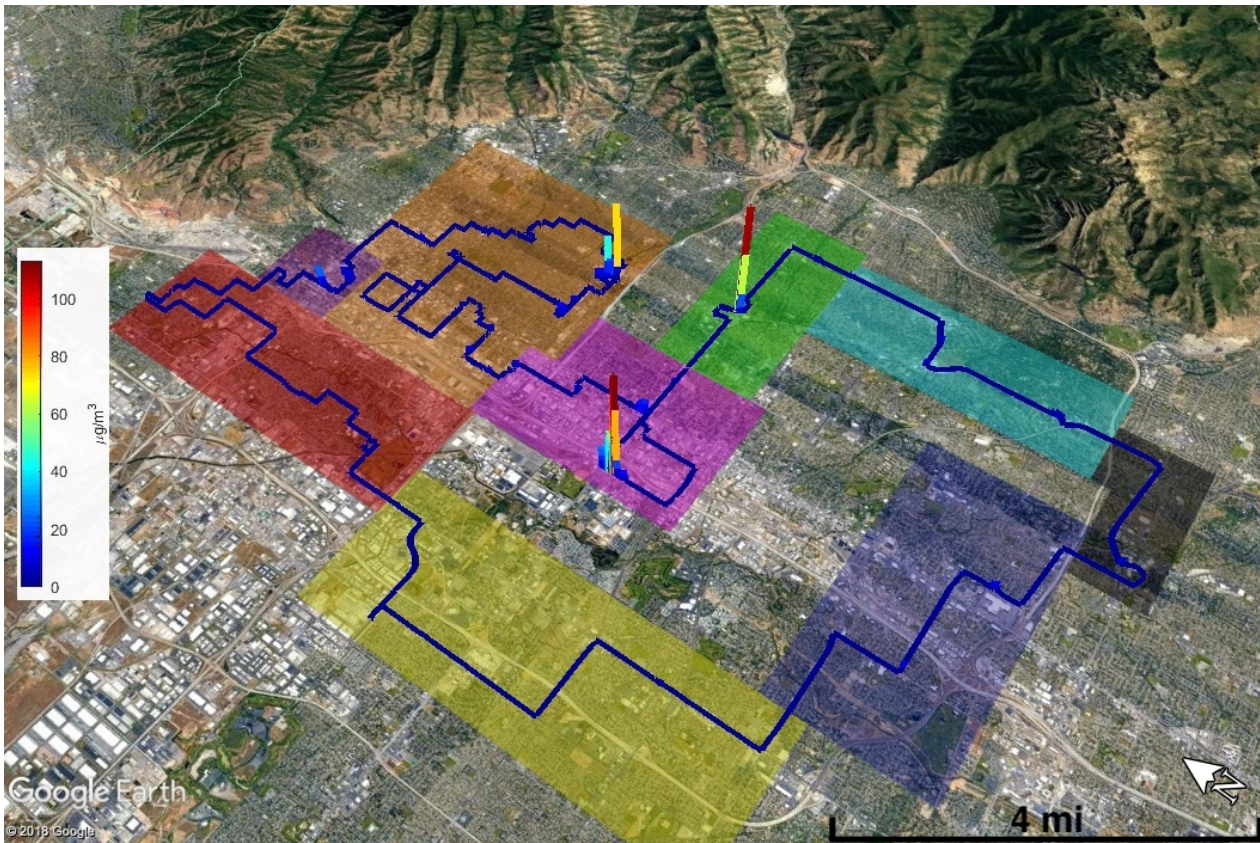


Figure 5: $PM_{2.5}$ data from January 16, 2019 mobile monitoring

Several large $PM_{2.5}$ peaks are immediately evident, while the remaining data shows no obvious activity. Consequently, the concentrations were rescaled to increase the resolution of smaller peaks as seen in Figure 6. The $PM_{2.5}$ concentrations of the largest peaks were reduced to increase resolution, therefore, the measured concentrations of these peaks are higher than depicted.

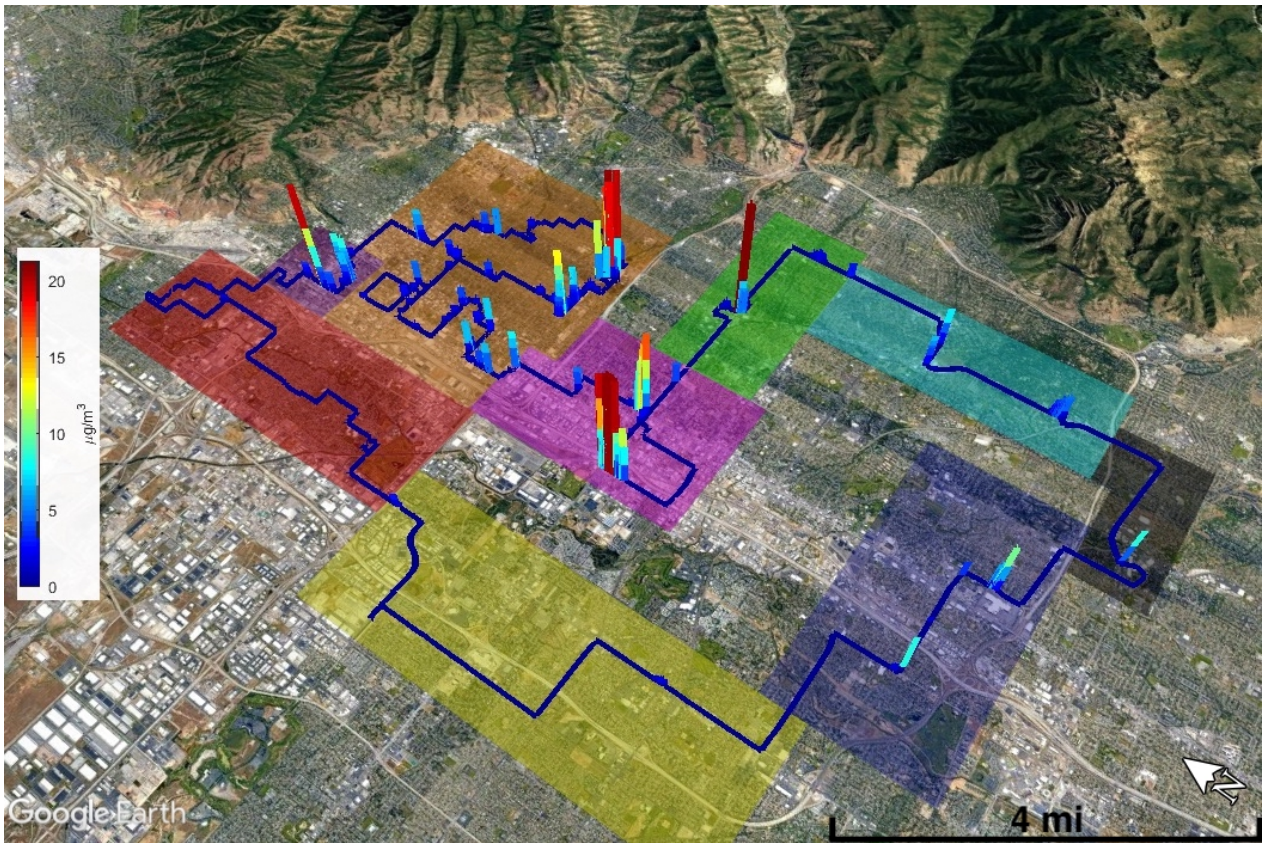


Figure 6: Increased resolution of PM_{2.5} concentrations from January 16, 2019 mobile monitoring

Similarly, the Delta-C values from the January 16, 2019 mobile monitoring were plotted as seen in Figure 7.

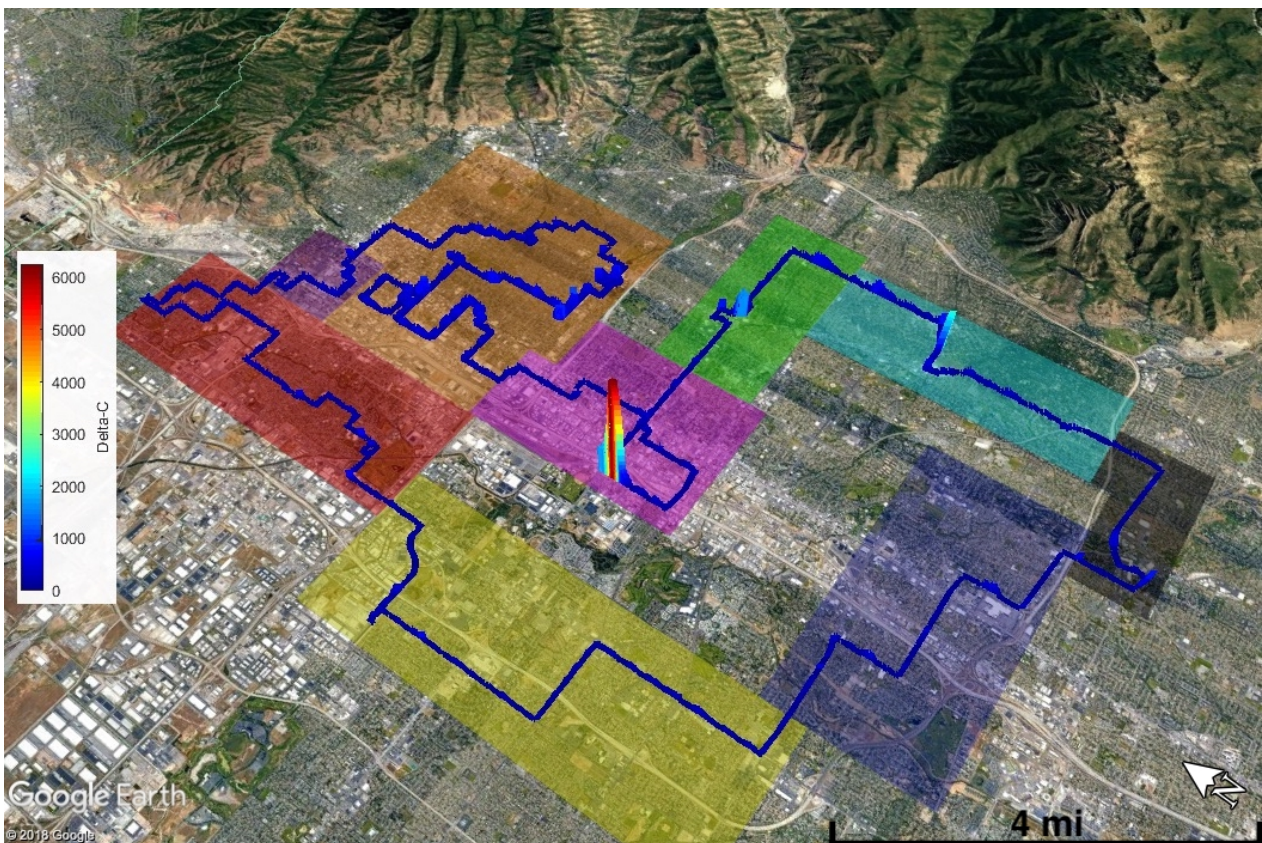


Figure 7: Delta-C measurements from January 16, 2019 mobile monitoring

The Delta-C results were rescaled to increase the resolution of smaller peaks as seen in Figure 8.

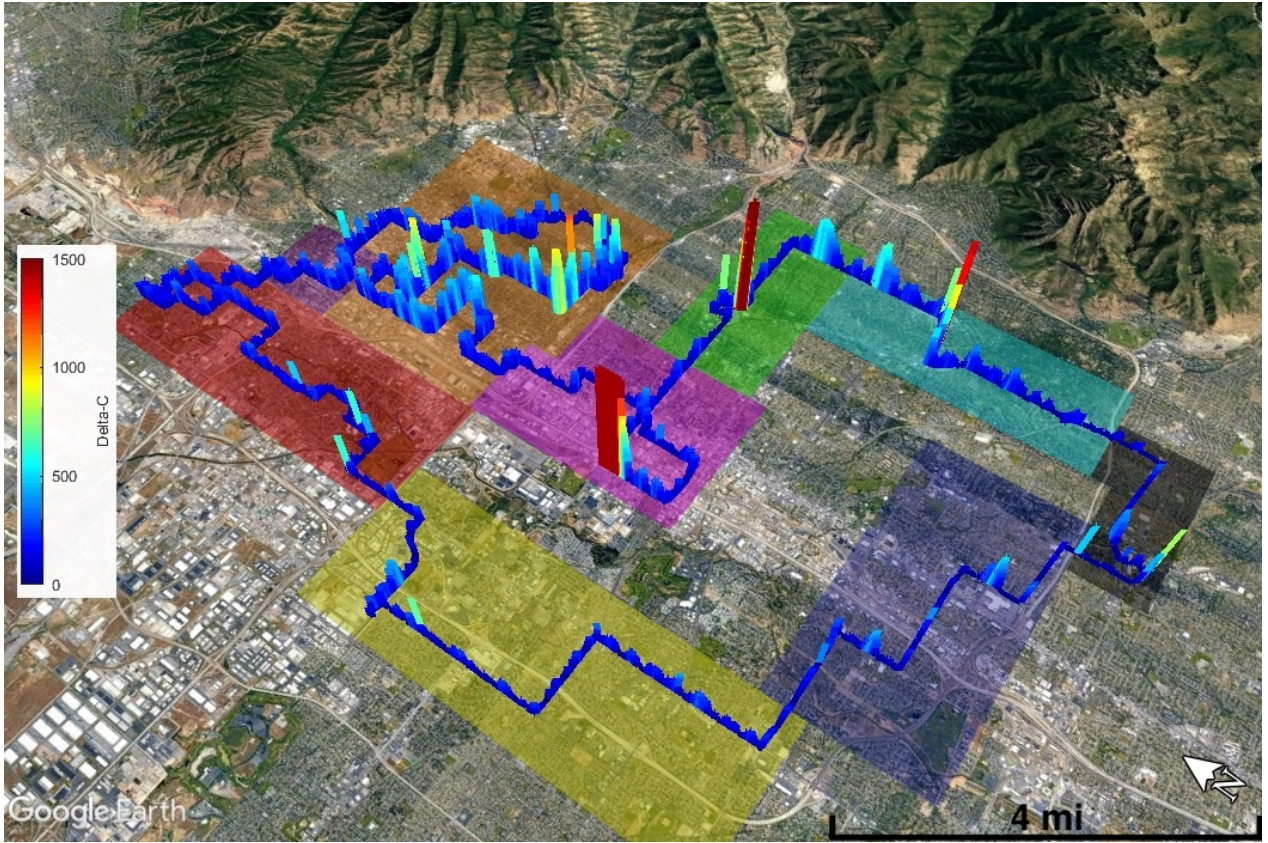


Figure 8: Increased resolution of Delta-C measurements from January 16, 2019 mobile monitoring

The mobile monitoring data was then automatically analyzed using a python script to objectively determine wood-burning events. For this process, the uncorrected DustTrak $PM_{2.5}$ data was used along with the smoothed aethalometer data. Each data set was considered to be a time series, with the time (t) ranging as integer values (\mathbb{Z}) from the first element to the total number of elements in the data set.

$$\{t \in \mathbb{Z} \mid 1 \leq t \leq n\} \quad (14)$$

First, the centered moving mean (z_t) was calculated throughout each data set using a 5-minute window ($\alpha = 300$ s) on either side of a given value (x_t) at time t . For the values not contained in the first and last 300 seconds of the data set, the moving mean calculation incorporated a total of 601 values. Near the beginning of each data set (first 300 points), fewer than 300 data points occurred prior to the value in question, therefore the mean was calculated with less than 601 data points. For example, the 10th data point was preceded by 9 values and followed by another 300 for a total of 310 data points involved in the mean calculation for x_{10} . Similarly, near the end of each data set (last 300 points), less than 300 points followed the value in question resulting in fewer than 601 points involved in the mean calculation. The equations for the moving mean calculations near the beginning, end, and center of the data set are shown below:

$$z_t = \begin{cases} \left(\frac{1}{\alpha + t} \right) \sum_{i=1}^{\alpha+t} x_i, & t \leq \alpha & \text{(First 300 Data Points)} \\ \left(\frac{1}{\alpha + (n-t) + 1} \right) \sum_{i=t-\alpha}^n x_i, & t \geq |n - \alpha| & \text{(Last 300 Data Points)} \\ \left(\frac{1}{2\alpha + 1} \right) \sum_{i=-\alpha}^{\alpha} x_{t+i}, & t = \alpha + 1, \alpha + 2, \dots, n - \alpha & \text{(Central Data Points)} \end{cases} \quad (15)$$

Using the same parameters, a centered moving standard deviation (σ_t) was calculated throughout each data set, which also incorporated fewer points into the calculation near the beginning and end of the data sets. The equations for calculating the moving standard deviation are shown below:

$$\sigma_t = \begin{cases} \sqrt{\frac{\sum_{i=1}^{\alpha+t} (x_i + z_t)^2}{\alpha + t - 1}}, & t \leq \alpha & \text{(First 300 Data Points)} \\ \sqrt{\frac{\sum_{i=t-\alpha}^n (x_i + z_t)^2}{\alpha + (n - t)}}, & t \geq |n - \alpha| & \text{(Last 300 Data Points)} \\ \sqrt{\frac{\sum_{i=-\alpha}^{\alpha} (x_{t+i} + z_t)^2}{2\alpha}}, & t = \alpha + 1, \alpha + 2, \dots, n - \alpha & \text{(Central Data Points)} \end{cases} \quad (16)$$

A threshold strategy was employed to objectively identify wood-burning events as an increase over baseline levels of PM_{2.5} and Delta-C. The first step in the threshold strategy was to create an estimate of baseline PM_{2.5} and Delta-C concentrations. The first attempt at estimating this baseline relied on an adjusted data set (y_t) that was created by removing values that differed from the mean by more than a standard deviation and replacing the removed values with the mean:

$$y_t = \begin{cases} z_t, & \text{if } |x_t - z_t| \geq \sigma_t \\ x_t, & \text{if } |x_t - z_t| < \sigma_t \end{cases} \quad (17)$$

The adjusted PM_{2.5} data set was then formatted into a .kmz file using the MATLAB script to obtain a visual representation using Google Earth:

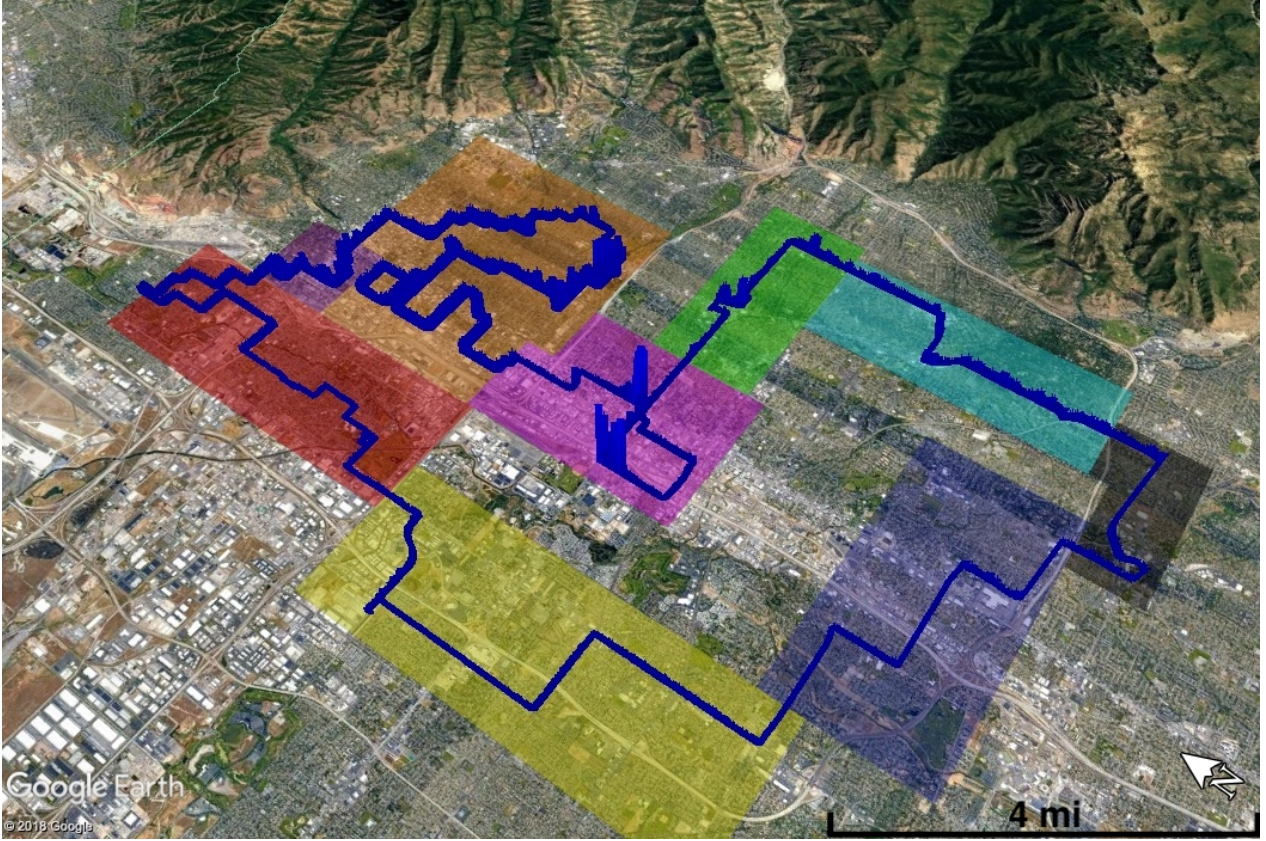


Figure 9: Adjusted January 16, 2019 PM_{2.5} data set

From visual inspection, it became obvious that some peaks still remained. Further investigation revealed that a high localized standard deviation prohibited the replacement of the elevated values. Therefore, a centered moving mean was applied to the adjusted data set to obtain the baseline (β_t), similar to Equation 15:

$$\beta_t = \begin{cases} \left(\frac{1}{\alpha + t} \right) \sum_{i=1}^{\alpha+t} y_i, & t \leq \alpha & \text{(First 300 Data Points)} \\ \left(\frac{1}{\alpha + (n-t) + 1} \right) \sum_{i=t-\alpha}^n y_i, & t \geq |n - \alpha| & \text{(Last 300 Data Points)} \\ \left(\frac{1}{2\alpha + 1} \right) \sum_{i=-\alpha}^{\alpha} y_{t+i}, & t = \alpha + 1, \alpha + 2, \dots, n - \alpha & \text{(Central Data Points)} \end{cases} \quad (18)$$

The data set obtained was sufficiently smooth to be used as a baseline for wood-burning event identification:

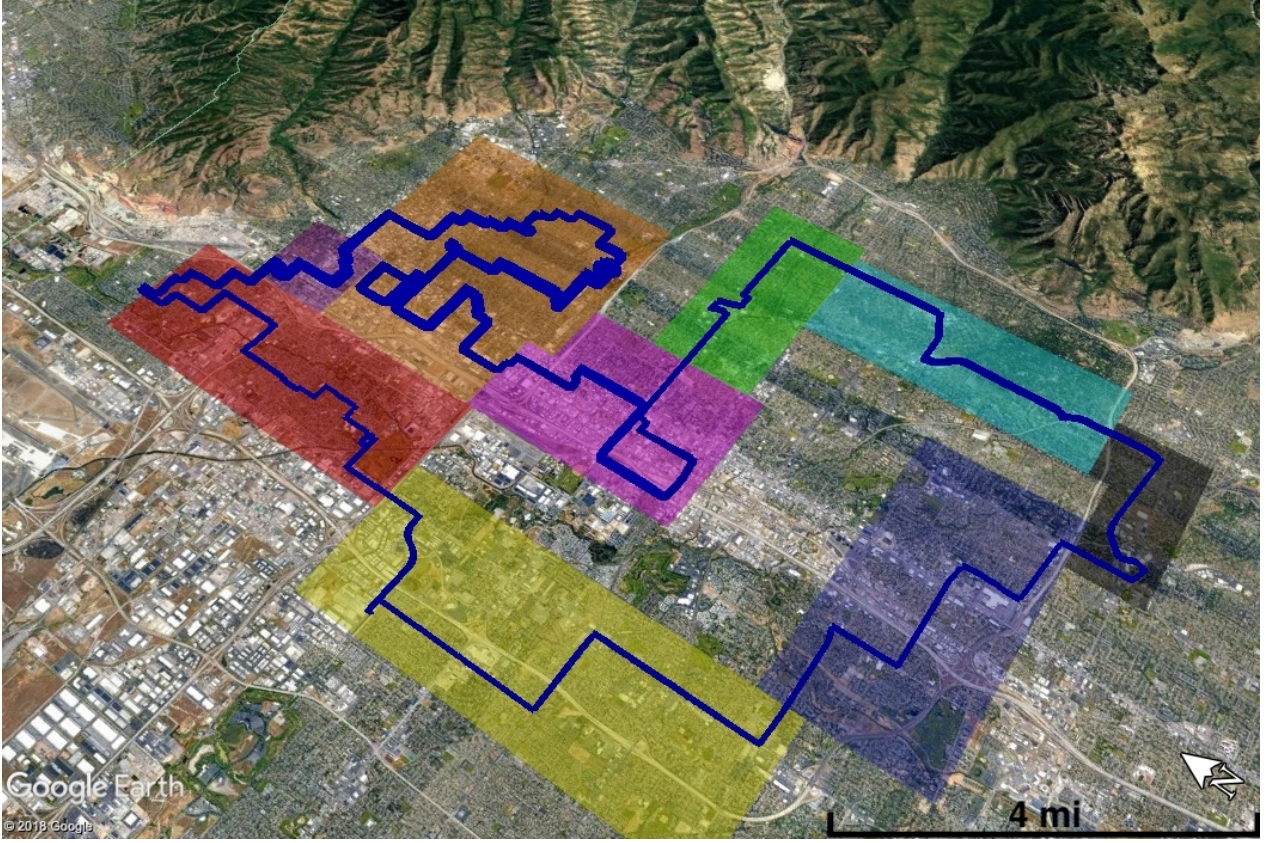


Figure 10: Baseline of January 16, 2019 PM_{2.5} data set

A wood-burning event was identified when both the PM_{2.5} and Delta-C values (x_t) exceeded their respective baseline by at least 2.5 standard deviations (σ_t). Because some of the PM_{2.5} peaks occurred only briefly, a 10-second buffer period (δ) was utilized on either side of a point where PM_{2.5} exceeded this criteria. Therefore, if both Delta-C (x^{DC}) and PM_{2.5} (x^{PM}) exceeded their corresponding baselines by 2.5 times the standard deviations of their respective data sets within a 21-second window, it was counted as a wood-burning event.

$$\left\{ \begin{array}{ll} \text{Event,} & \text{if } |x_t^{PM} - \beta_t^{PM}| \geq (2.5 * \sigma_t^{PM}) \\ & \text{and } |x_{t+\delta}^{DC} - \beta_{t+\delta}^{DC}| \geq (2.5 * \sigma_{t+\delta}^{DC}) \\ \text{No Event,} & \text{otherwise} \end{array} \right. \quad (19)$$

where

$$\{t \in \mathbb{Z} \mid 1 \leq t \leq n\} \quad (20)$$

$$\{\delta \in \mathbb{Z} \mid -10 \leq \delta \leq 10\} \quad (21)$$

The wood-burning events were then classified by region in which they occurred to provide insight to spatial trends.

Deviations

Due to the damaged glass air sampling manifold at the Rose Park DAQ air monitoring station, the Rose Park aethalometer data was not included in the study. Prior to the commencement of mobile monitoring, a tentative driving schedule was submitted to the DAQ. This schedule was later modified based on inclement weather, air quality conditions, and staff availability. The modified driving schedule acknowledged the goals of the project, and ensured that data collection occurred over an acceptable distribution of days of the week, air quality conditions, and residential wood-burning restrictions.

Results

Stationary Monitoring

Figure 11 shows an example of the Delta-C measurements from the Smithfield air monitoring station for the month of December 2018 versus the 24-hour heat deficit over the same time period.

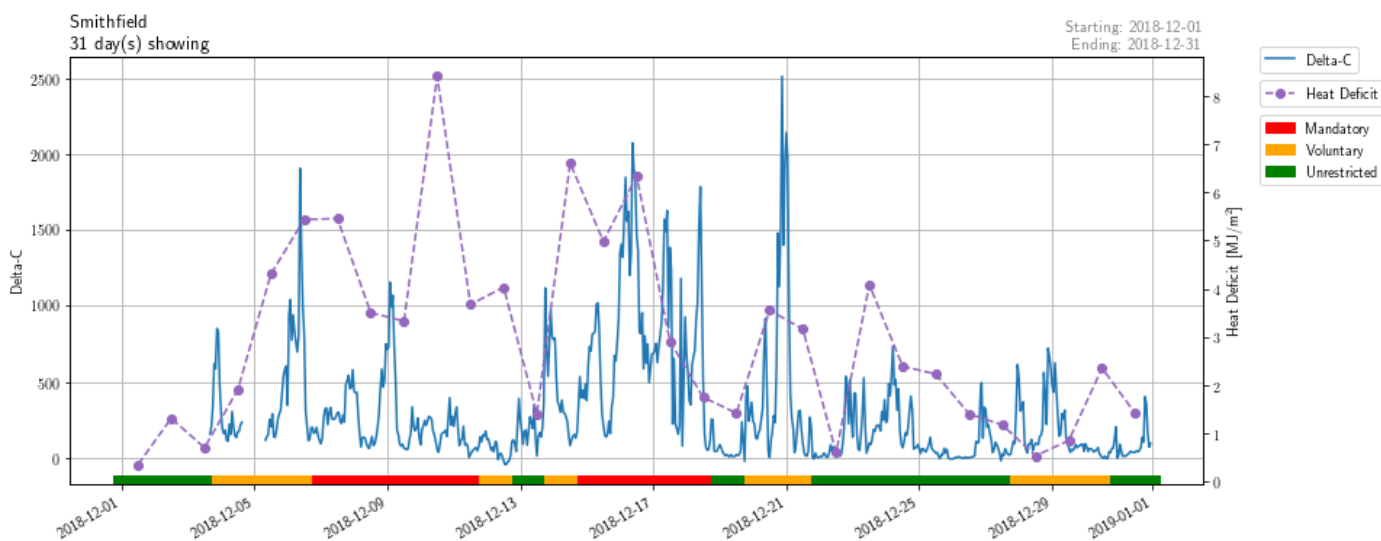


Figure 11: Smithfield Delta-C and heat deficit December 2018

Note that a portion of the Delta-C data is missing because the Smithfield aethalometer was not functioning properly for the first several days in December. The color bar along the x-axis represents the residential wood-burning restrictions in Cache County. The DAQ implements wood-burning restrictions when poor air quality is expected, which generally occurs as a result of PCAPs during the winter months. Elevated Delta-C values occurring during periods of a relatively high heat deficit is suggestive of wood-burning contributions despite DAQ restrictions. This behavior is consistent with the trends observed in Figure 11. The Delta-C and PM_{2.5} concentrations obtained from the Smithfield air monitoring station for the month of December 2018 can be seen in Figure 12.

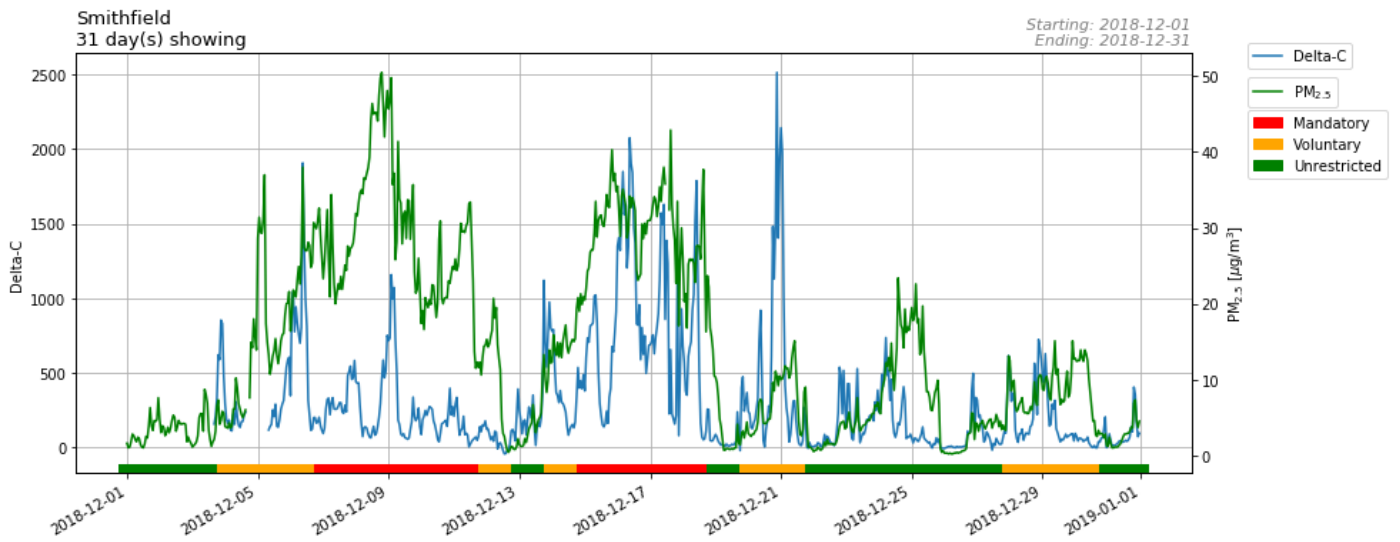


Figure 12: Smithfield Delta-C and PM_{2.5} December 2018

Several of the PM_{2.5} peaks are accompanied by a corresponding Delta-C peak, which suggests that a portion of the elevated PM_{2.5} levels can be attributed to biomass combustion. The elevated PM_{2.5} levels generally occur on “mandatory action” days, which is consistent with expectations. Figure 13 shows the Delta-C and temperature data obtained from the Smithfield air monitoring station for the month of December 2018.

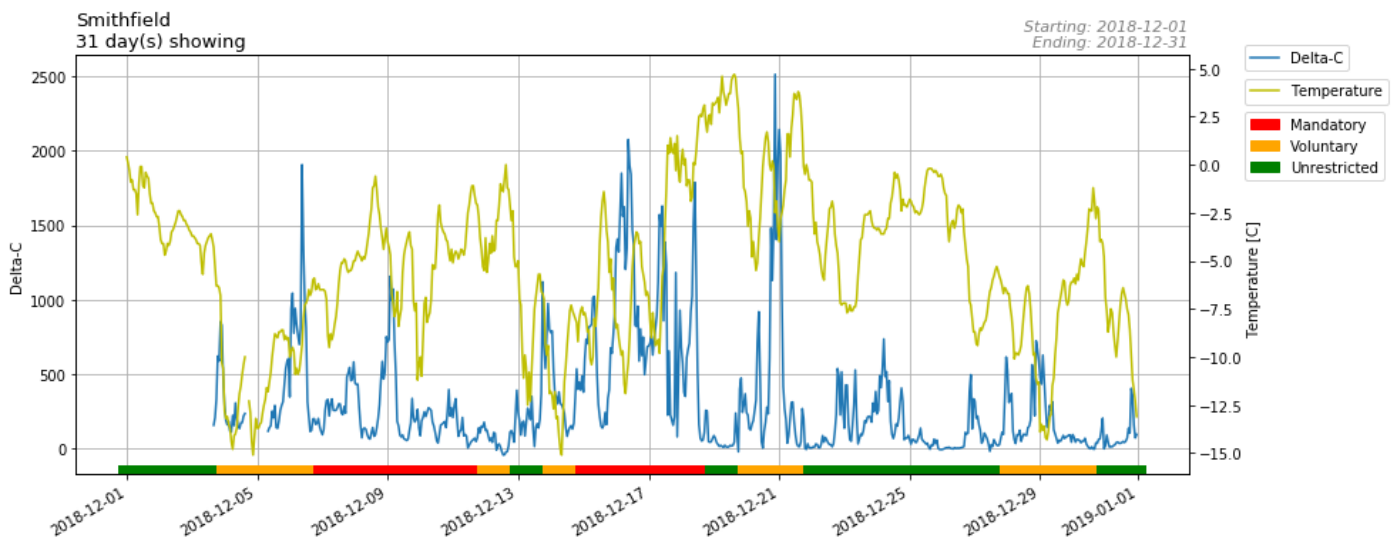


Figure 13: Smithfield Delta-C and temperature (°C) December 2018

Some of the Delta-C peaks occurred during a corresponding drop in temperature, which is consistent with the expectation to observe increased residential wood-burning during periods of reduced temperature. Note that the monthly graphs of Delta-C with heat deficit, PM_{2.5}, and temperature for all three monitoring stations can be found in Appendix B: Stationary Monitoring.

A threshold was implemented to determine trends corresponding to the day of the week on which wood-burning occurrences were more frequent. In the event that a Delta-C 1-minute average exceeded 750 ng/m³ at any of the stationary monitoring locations, a wood-burning event was considered to have occurred. To reduce

the possibility of over-counting, a single event was considered when a prolonged period of 1-minute averages greater than the threshold occurred. In the event that an exceedance occurred for an extended period of time, the event was counted at the first moment that the threshold was reached. The count of these exceedances is shown in Figure 14 for Bountiful (BV), Lindon (LN), and Smithfield (SM). The data set was further broken down based on residential wood-burning restrictions as seen in Figures 15-17.

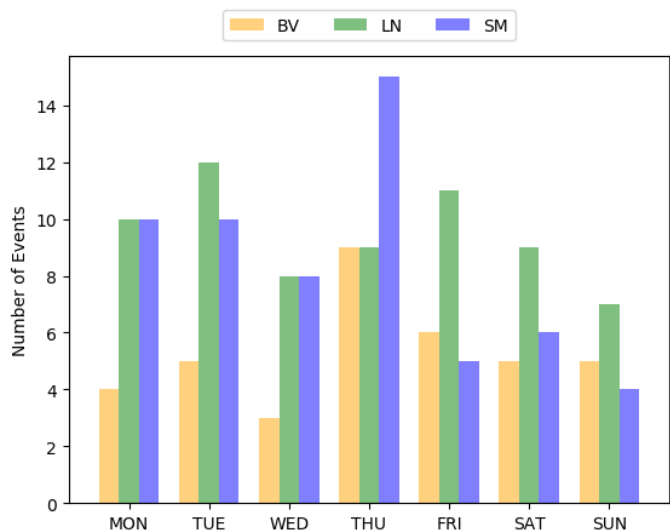


Figure 14: Delta-C threshold exceedances

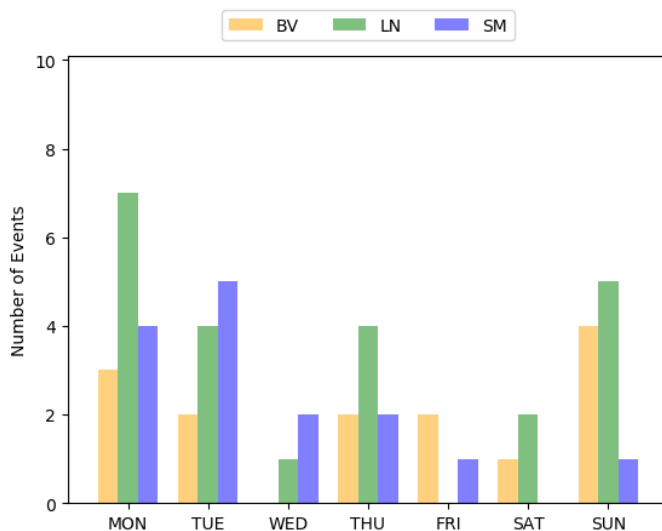


Figure 15: Unrestricted Action

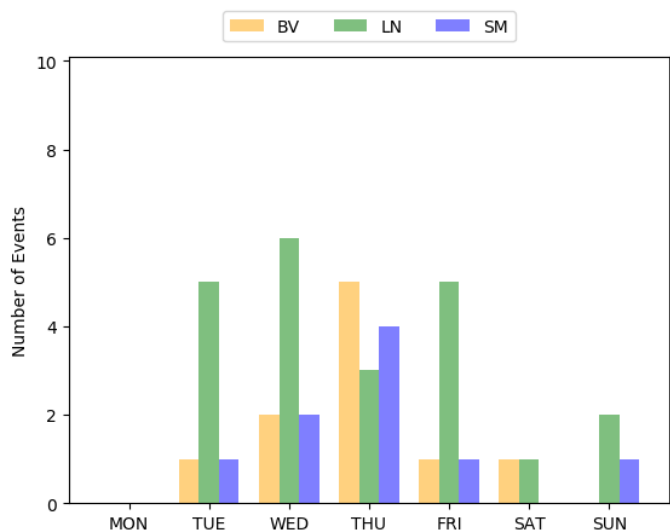


Figure 16: Voluntary Action

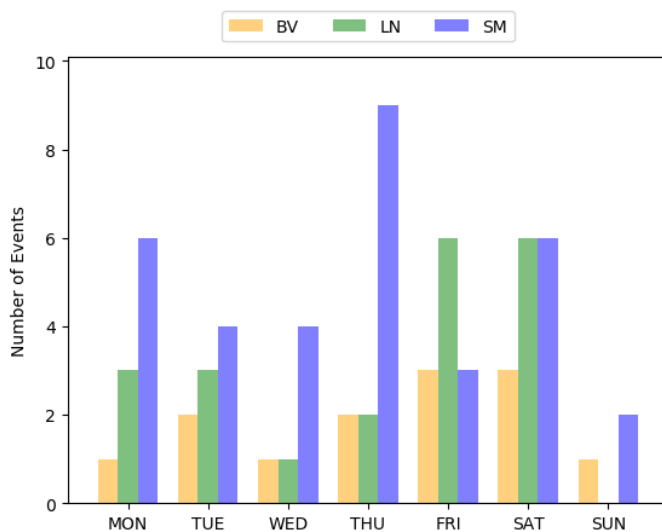


Figure 17: Mandatory Action

Irrespective of restrictions, the majority of exceedances at the Bountiful monitoring station occurred from Thursday-Sunday, which was consistent with expectations to observe increased wood-burning during weekends. Smithfield exhibited contrasting results with the majority of events occurring from Monday-Thursday, while Lindon showed a fairly even distribution throughout the week. During “Mandatory Action” days, all three locations displayed relatively increased wood-burning on weekends.

The Delta-C exceedances were also plotted by the hour of day in which they occurred as seen in Figures 18-

21. Irrespective of restrictions, over 50% of the events at all monitoring stations occurred between 5 pm and 11 pm, which is consistent with expectations to observe increased wood-burning during evenings. All three stations also showed a decrease in wood-burning during the middle of the day from 11 am to 4 pm. On “Mandatory Action” days, at least half of the threshold exceedances occurred between 5 pm and 11 pm at all three stations, which demonstrates a disregard for residential wood-burning restrictions.

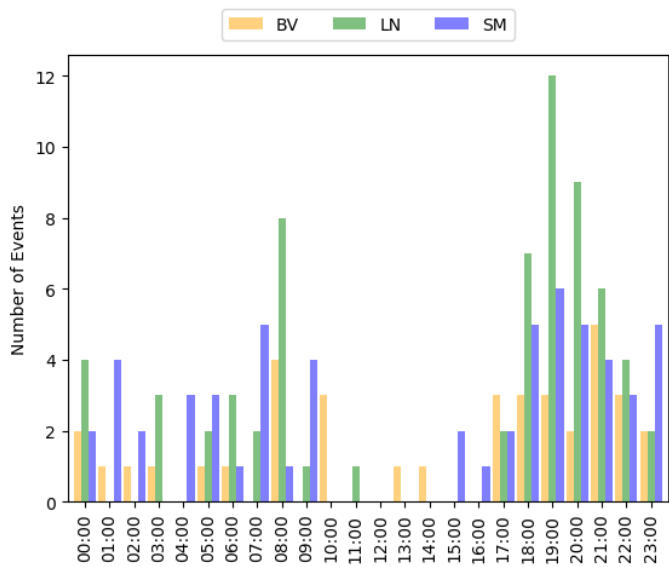


Figure 18: Delta-C threshold exceedances

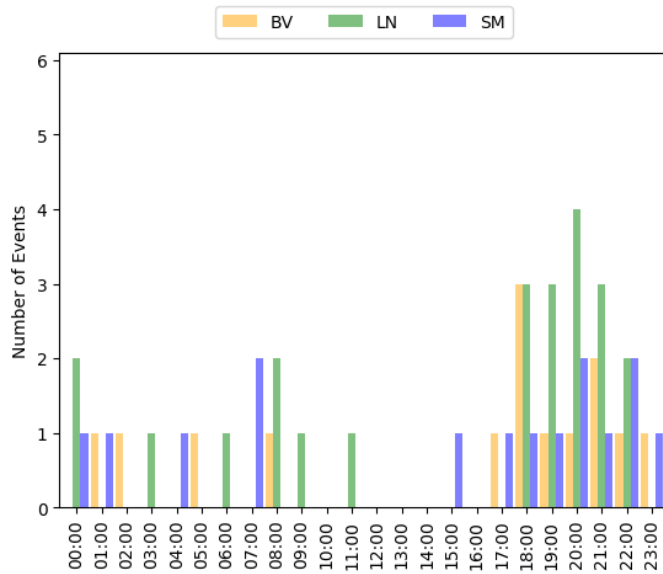


Figure 19: Unrestricted Action

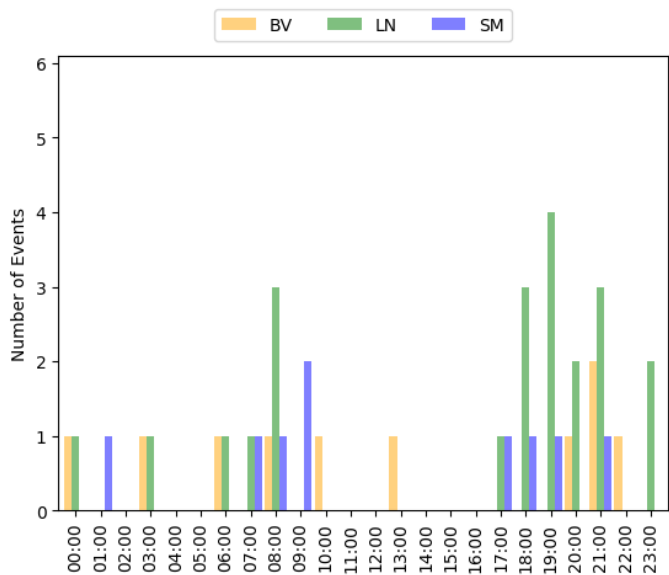


Figure 20: Voluntary Action

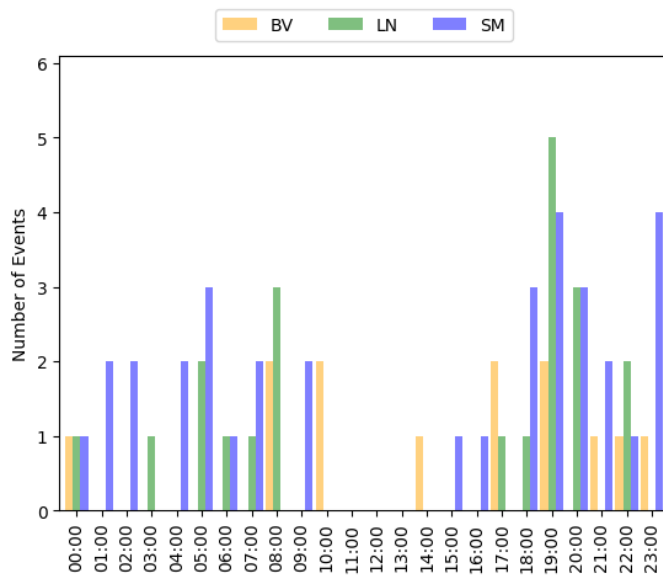


Figure 21: Mandatory Action

Mobile Monitoring

Throughout the mobile monitoring data collection period, several commercial and residential locations were observed to have frequent wood-burning regardless of residential wood-burning restrictions. Figure 22 shows the $PM_{2.5}$ data from Wednesday, January 16, 2019 with rescaled values of the larger peaks to increase resolution. January 16 was classified as a "unrestricted action" day by DAQ residential wood-burning restrictions in Salt Lake County.

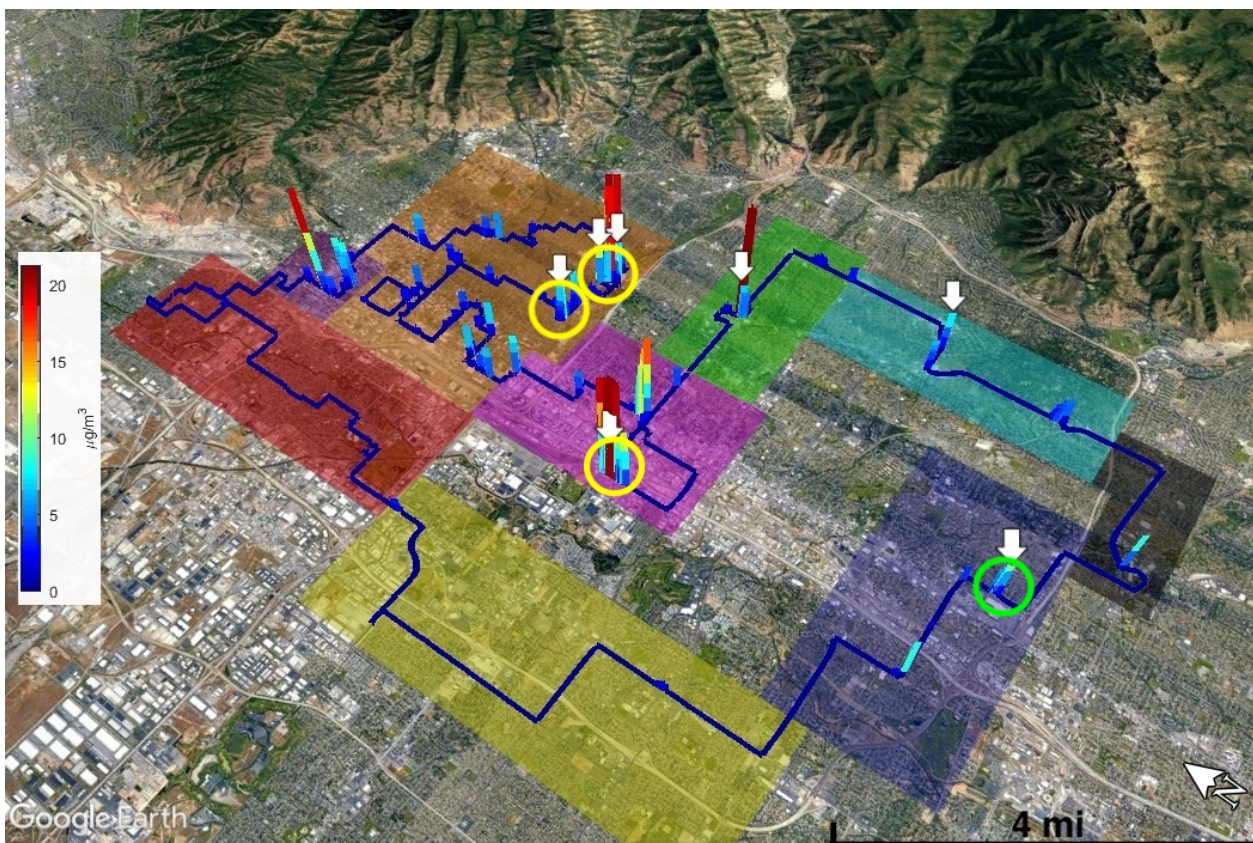


Figure 22: Wednesday, January 16, 2019 $PM_{2.5}$ data with common wood-burning locations

The yellow and green circles correspond to commercial and residential locations that often exhibited wood-burning. For eight of the twelve mobile sampling days, the largest $PM_{2.5}$ or Delta-C values observed can be attributed to emissions from one of these four circled locations. The wood-burning events determined by the Python script are denoted with white arrows, and on this date, four of the seven events occurred at these locations. Wood-burning was also noted at the same four locations on Tuesday, February 12, 2019, which was classified as a "voluntary action" day in Salt Lake County. "Voluntary action" in Salt Lake County is treated as "mandatory action", meaning that residential wood-burning is prohibited. Figure 23 shows the $PM_{2.5}$ data from February 12, which is rescaled values to increase resolution.

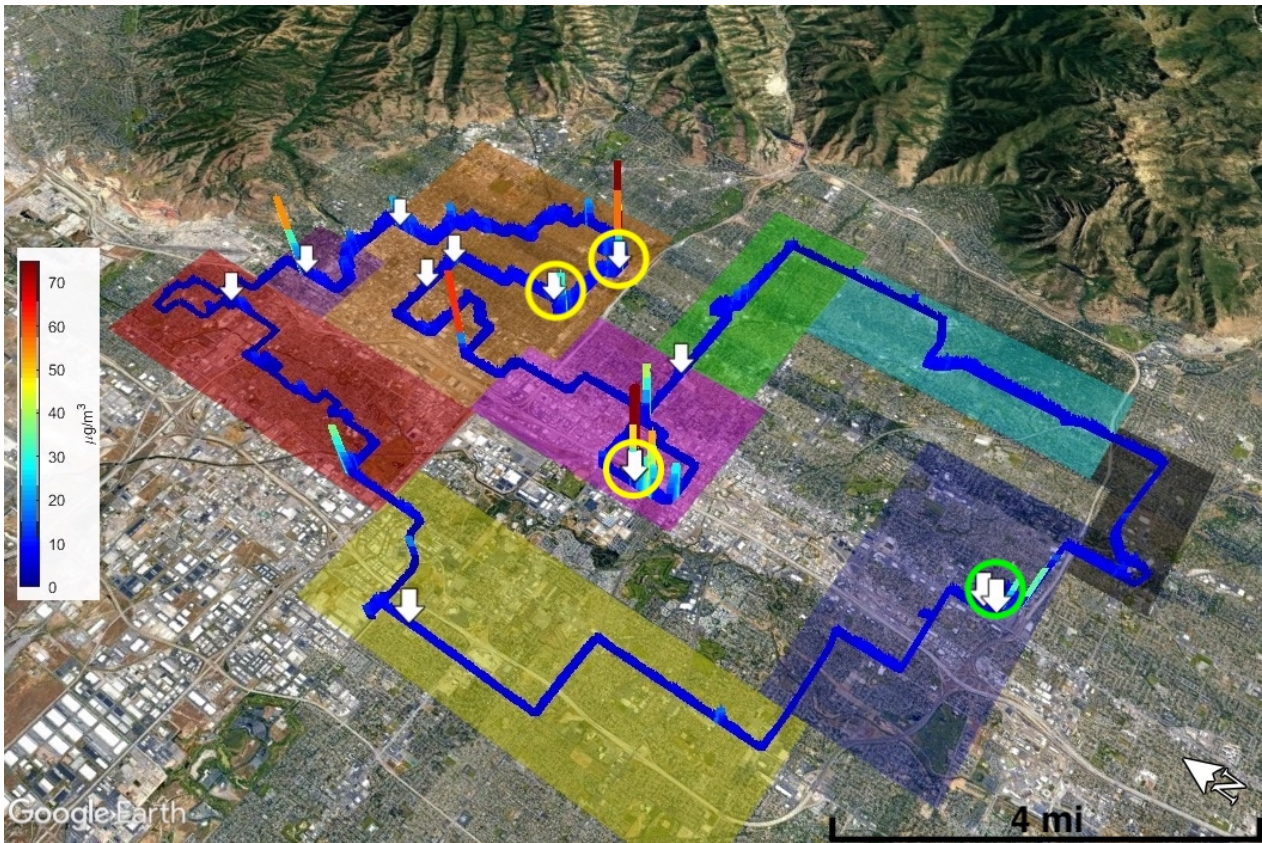


Figure 23: Tuesday, February 12, 2019 PM_{2.5} data with common wood-burning locations

In contrast, on Friday, February 1, 2019 (Figure 24), the consistent residential wood-burning location was identified, while the three commercial locations were not. Significant residential wood-burning was observed regardless of the “mandatory action” designation in Salt Lake County. The background PM_{2.5} levels were notably higher, which is consistent with a PCAAP event.

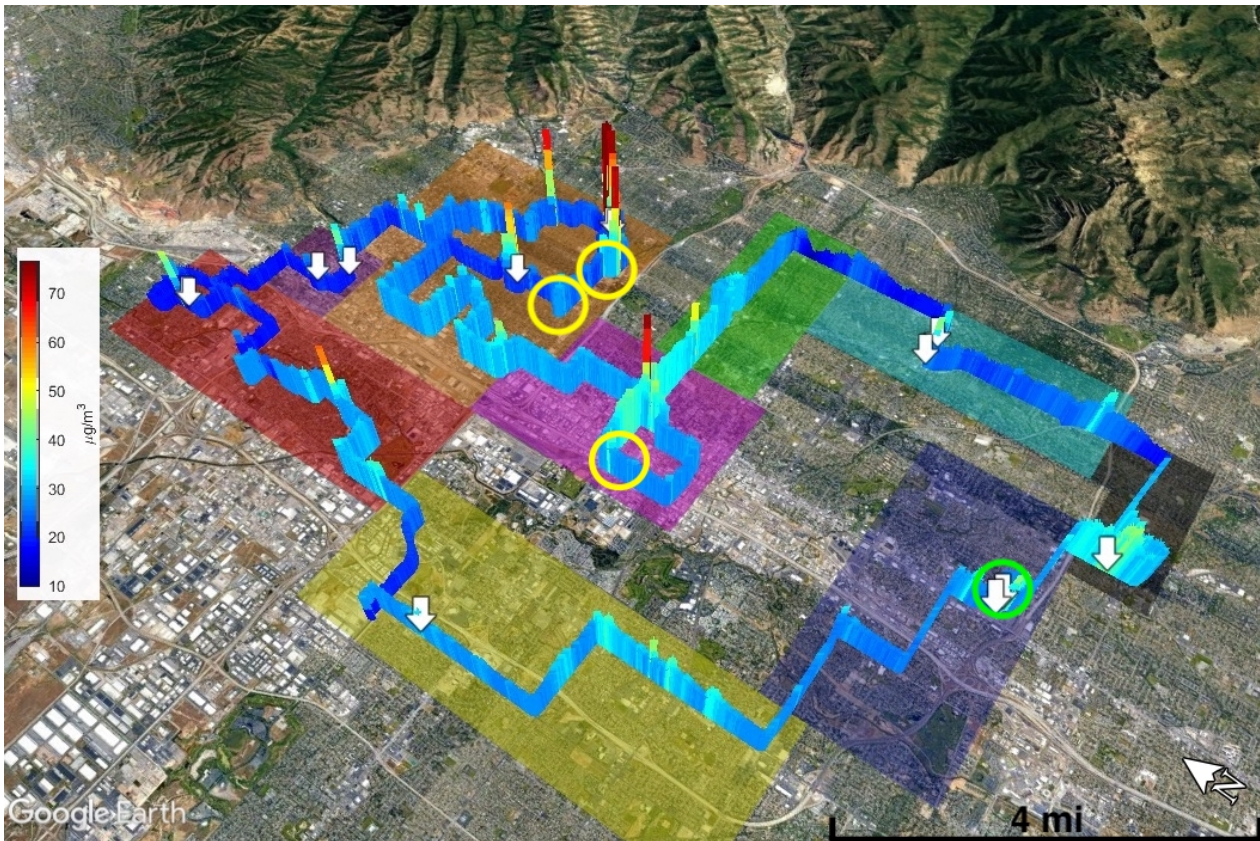


Figure 24: Friday, February 1, 2019 PM_{2.5} data with common wood-burning locations

For all sampling days, the mobile monitoring plots of PM_{2.5}, Delta-C, and Delta-C with identified wood-burning events can be found in Appendix B: Mobile Monitoring.

The total number of wood-burning events from all 12 sampling periods were separated by region as seen in Figure 25. The “Boundary-Case Events” in the West Valley region are a count of the peaks that occurred within the first and last 300 seconds of sampling. The validity of these events is less certain because fewer points were used to calculate the moving mean, standard deviation, and baseline, therefore the criteria for classification as a wood-burning event was more easily attained.

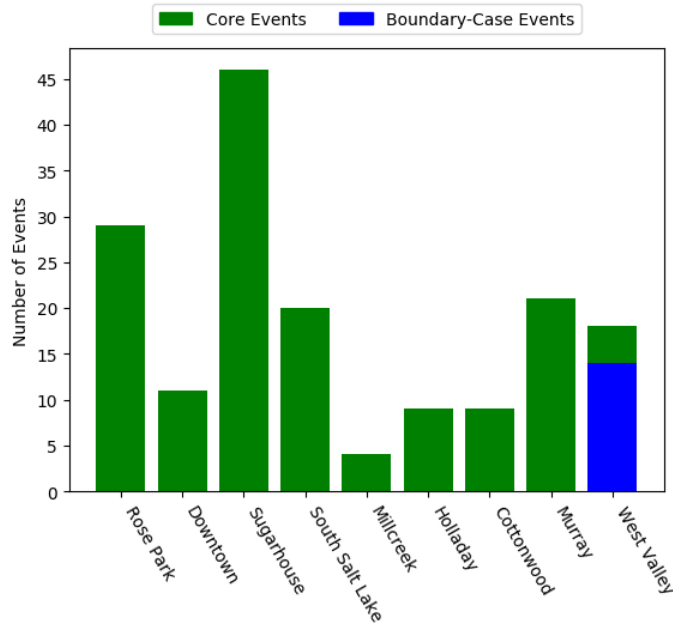


Figure 25: Cumulative wood-burning event counts per region

The highest number of events occurred in Sugarhouse, however, this was the largest region where the most sampling time occurred, as seen in Figure 26. To gain a better understanding of wood-burning events likely to be found in each region, the cumulative count of event occurrences in a region was normalized by the time spent in the region as seen in Figure 27.

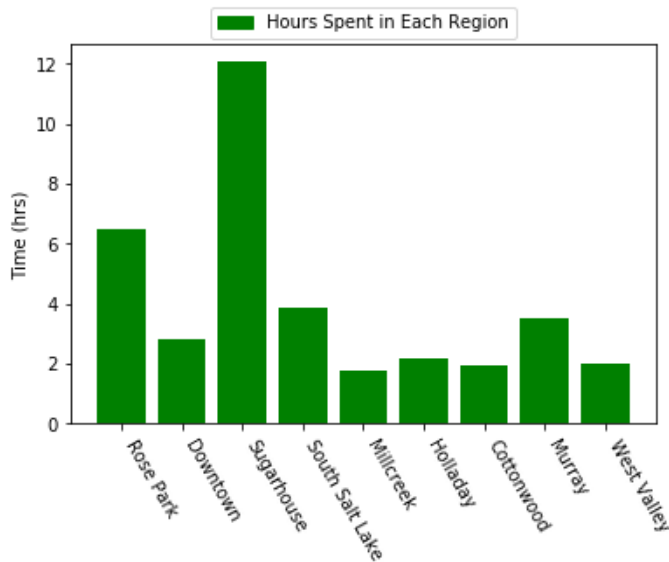


Figure 26: Cumulative time per region

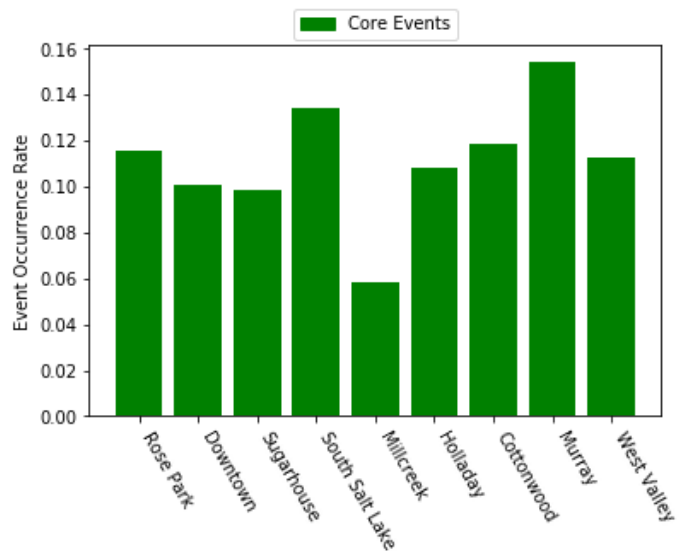


Figure 27: Time-normalized events

If the mobile sampling were to be replicated by driving along the same route, Figure 27 serves as an indication of the distribution of events likely to be encountered while spending a given amount of time in each region. Although the count of Sugarhouse wood-burning events was more than double the counts found in Downtown, Murray, and South Salt Lake, each of these regions actually had greater event frequency than Sugarhouse per sampling time in the region.

Conclusions

Analysis of the stationary data indicates wood burning occurs during “mandatory action” periods at all three monitoring stations. In addition, wood-burning events in Bountiful tended to occur more frequently during weekends. The mobile monitoring results further suggest lack of compliance with residential wood-burning restrictions, with numerous incidents of residential wood-burning despite during “mandatory action” periods. On three of the twelve driving days (one “voluntary action” day and two “mandatory action” days), the most substantial wood-burning event was likely attributable to a commercial location. While restaurants and institutional food preparation facilities are exempt from burn restrictions, the mobile monitoring data suggests that these commercial locations are contributing to elevated $PM_{2.5}$ levels during poor air quality events.

Archive of Data and Results

The stationary data is available through an online tool (described in the following section), and the mobile data is available at the following publicly available drive:

<https://drive.google.com/drive/u/0/folders/1HGJikl6sayvx1S74bKb01bqrcVfEhO0T>

The files are organized by sampling date. The csv files contain the time-synchronized aethalometer and Dust-Trak data, and the files labeled plot.xls contain the corrected DustTrak and Delta-C data that are plotted on the maps. The kmltoolbox and the files with the .m (Matlab extensions) can be used to generate the maps shown in this report, and the kmz files are the map files.

Online Delta Carbon Tool

It will be useful to continue evaluating Delta-C at the locations where the aethalometers are located. An online tool was developed to collect, process, and generate heat deficit and Delta-C for the Smithfield, Bountiful, and Lindon locations. This tool contains available historical data, and it will continue to automatically update as long as the DAQ data feed continues from the same source. The tool will generate figures such as Figure 11 - 13 for selected dates and locations. This tool is available at:

<https://kelly-1.chemeng.utah.edu/>

Future Directions

While this study provided insight into wood-burning contributions to $PM_{2.5}$ and compliance with wood-burning restrictions along the Wasatch Front, more conclusive results could be achieved with more prolonged sampling. Analyzing the stationary monitoring data collected over a period of several years rather than months would likely make trends more obvious, reduce variability, and help to identify long-term trends. Redeploying the

aethalometer at Rose Park would provide valuable data for the Salt Lake City air shed. Extending the stationary monitoring would be facilitated by the Python scripts developed under this project that automatically collect the online data files and produce Delta-C plots. The mobile monitoring could also be expanded to other areas including Bountiful, Ogden/Provo, and elsewhere within the nonattainment areas. While mobile monitoring is undoubtedly more expensive and resource intensive, having a larger data set would also be beneficial to understanding the contributions of commercial wood burning.

References

- ¹ C. David Whiteman, Xindi Bian, and Shiyuan Zhong. Wintertime Evolution of the Temperature Inversion in the Colorado Plateau Basin, 1999.
- ² Geoffrey D. Silcox, Kerry E. Kelly, Erik T. Crosman, C. David Whiteman, and Bruce L. Allen. Winter-time PM 2.5 concentrations during persistent, multi-day cold-air pools in a mountain valley. *Atmospheric Environment*, 46:17–24, 2012.
- ³ PM2.5 State Implementation Plans (SIPs) 2018 State of the Environment Report (AQ) - Utah Department of Environmental Quality. <https://deq.utah.gov/communication/state-of-the-environment-report/pm2-5-state-implementation-plans-sips-2018-state-of-the-environment-report-aq> [Accessed: April, 2019].
- ⁴ PM2.5 Overview - Particulate Matter - Division of Air Quality - Utah Department of Environmental Quality. <https://deq.utah.gov/legacy/pollutants/p/particulate-matter/pm25/index.htm> [Accessed: April, 2019].
- ⁵ Francis J. Ries, Julian D. Marshall, and Michael Brauer. Intake fraction of urban wood smoke. *Environmental Science and Technology*, 43(13):4701–4706, 2009.
- ⁶ A. Kocbach, B. V. Johansen, P. E. Schwarze, and E. Namork. Analytical electron microscopy of combustion particles: A comparison of vehicle exhaust and residential wood smoke. *Science of the Total Environment*, 346(1-3):231–243, 2005.
- ⁷ Tracy L. Thatcher, Thomas W. Kirchstetter, Christopher J. Malejan, and Courtney E. Ward. Infiltration of Black Carbon Particles from Residential Woodsmoke into Nearby Homes. *Open Journal of Air Pollution*, 03(04):111–120, 2014.
- ⁸ Robert Kotchenruther (EPA Region 10). Source Apportionment of PM2.5 at Three Urban Sites Along Utah’s Wasatch Front. 2011.
- ⁹ Kerry E. Kelly, Robert Kotchenruther, Roman Kuprov, and Geoffrey D. Silcox. Receptor model source attributions for Utah’s Salt Lake City airshed and the impacts of wintertime secondary ammonium nitrate and ammonium chloride aerosol. *Journal of the Air and Waste Management Association*, 63(5):575–590, 2013.
- ¹⁰ ADA Hansen, H Rosen, and T Novakrov. The Aethalometer - an instrument for the real-time measurement of optical absorption by aerosol particles. *Science of the Total Environment*, 36:191–196, 1984.
- ¹¹ Qian Zhang, Zhenxing Shen, Yali Lei, Yueshe Wang, Yaling Zeng, Qiyuan Wang, Zhi Ning, Junji Cao, Linqing Wang, and Hongmei Xu. Variations of particle size distribution, black carbon, and brown carbon during a severe winter pollution event over Xi’an, China. *Aerosol and Air Quality Research*, 18(6):1419–1430, 2018.

- ¹² X. F. Huang, R. S. Gao, J. P. Schwarz, L. Y. He, D. W. Fahey, L. A. Watts, A. McComiskey, O. R. Cooper, T. L. Sun, L. W. Zeng, M. Hu, and Y. H. Zhang. Black carbon measurements in the Pearl River Delta region of China. *Journal of Geophysical Research Atmospheres*, 116(12):1–10, 2011.
- ¹³ Yunfei Wu, Xiaojia Wang, Jun Tao, Rujin Huang, Ping Tian, Junji Cao, Leiming Zhang, Kin Fai Ho, Zhiwei Han, and Renjian Zhang. Size distribution and source of black carbon aerosol in urban Beijing during winter haze episodes. *Atmospheric Chemistry and Physics*, 17(12):7965–7975, 2017.
- ¹⁴ Qian Zhang, Zhi Ning, Zhenxing Shen, Guoliang Li, Junke Zhang, Yali Lei, Hongmei Xu, Jian Sun, Leiming Zhang, Dane Westerdahl, Nirmal Kumar Gali, and Xuesong Gong. Variations of aerosol size distribution, chemical composition and optical properties from roadside to ambient environment: A case study in Hong Kong, China. *Atmospheric Environment*, 166:234–243, 2017.
- ¹⁵ E. Weingartner, H. Saathoff, M. Schnaiter, N. Streit, B. Bitnar, and U. Baltensperger. Absorption of light by soot particles: Determination of the absorption coefficient by means of aethalometers. *Journal of Aerosol Science*, 34(10):1445–1463, 2003.
- ¹⁶ L. Drinovec, G. Močnik, P. Zotter, A. S.H. Prévôt, C. Ruckstuhl, E. Coz, M. Rupakheti, J. Sciare, T. Müller, A. Wiedensohler, and A. D.A. Hansen. The “dual-spot” Aethalometer: An improved measurement of aerosol black carbon with real-time loading compensation. *Atmospheric Measurement Techniques*, 8(5):1965–1979, 2015.
- ¹⁷ Magee Scientific. Aethalometer ® Model AE33 User Manual. (January):1–68, 2017.
- ¹⁸ Aki Virkkula, Timo Mäkelä, Risto Hillamo, Tarja Yli-Tuomi, Anne Hirsikko, Kaarle Hämeri, and Ismo K. Koponen. A simple procedure for correcting loading effects of aethalometer data. *Journal of the Air and Waste Management Association*, 57(10):1214–1222, 2007.
- ¹⁹ K. Max Zhang, George Allen, Bo Yang, Geng Chen, Jiajun Gu, James Schwab, Dirk Felton, and Oliver Rattigan. Joint measurements of PM_{2.5} and light-absorptive PM in woodsmoke-dominated ambient and plume environments. *Atmospheric Chemistry and Physics*, 17(18):11441–11452, 2017.
- ²⁰ George Allen, Peter Babich, and Richard L. Poirot. Evaluation of a New Approach for Real Time Assessment of Wood Smoke PM. *Air & Waste Management Association Visibility Specialty Conference on Regional and Global Perspectives on Haze: Causes, Consequences and Controversies*, pages 1–11, 2004.
- ²¹ Yungang Wang, Philip K Hopke, Oliver V Rattigan, Xiaoyan Xia, David C Chalupa, and Mark J Utell. Characterization of Residential Wood Combustion Particles Using the. *Environmental Science & Technology*, 45:7387–7393, 2011.

- ²² Connecticut Department of Environmental Protection, Bureau of Air Management (2011). Evaluation of Wood Smoke Contribution to Particle Matter in Connecticut Connecticut Department of Environmental Protection Bureau of Air Management. http://www.ct.gov/deep/lib/deep/air/wood_stove_furnaces/ctdep_woodsmokefinalreport.pdf.
- ²³ C. David Whiteman, Sebastian W. Hoch, John D. Horel, and Allison Charland. Relationship between particulate air pollution and meteorological variables in Utah's Salt Lake Valley. *Atmospheric Environment*, 94:742–753, 2014.
- ²⁴ Gray Bertelsen, Bethany Crowley, Jason McHann, and Melissa Puga. Wintertime Characteristics of PM_{2.5} in the Salt Lake Valley. pages 1–27, 2016.